



Available online at [www.sciencedirect.com](http://www.sciencedirect.com)



Engineering Failure Analysis 12 (2005) 337–347

---

**ENGINEERING  
FAILURE  
ANALYSIS**

---

[www.elsevier.com/locate/engfailanal](http://www.elsevier.com/locate/engfailanal)

## Cracking in cargo aircraft main landing gear truck beams due to abusive grinding following chromium plating

Noam Eliaz <sup>a,\*</sup>, Haim Sheinkopf <sup>b</sup>, Gil Shemesh <sup>b</sup>, Hillel Artzi <sup>b</sup>

<sup>a</sup> *Biomaterials and Corrosion Laboratory, Department of Solid Mechanics, Materials and Systems,  
Tel-Aviv University, Tel-Aviv 69978, Israel*

<sup>b</sup> *Depot 22, Materials Division, Israel Air Force, P.O. Box 02548, Israel*

Accepted 10 October 2004

Available online 11 November 2004

---

### Abstract

While a wheel was being replaced on the subject aircraft, a crack was found on the rear axle bore of the left-hand main landing gear truck beam. This part had been overhauled 11 months earlier. One year later, while the subject aircraft was being parked, two loud bangs were heard coming from the right-hand main landing gear. Upon inspection, the right-hand truck beam was found cracked longitudinally at two locations on the rear axle bore. Microscopic examination revealed two crack origins, one on each side of the bore. Both cracks propagated from corrosion pits under the chromium plating in a stable intergranular mechanism. The final overload fracture produced quasi-cleavage features. Nital etch, following removal of the chromium plating, revealed areas of overtempered and untempered martensite indicative of heat damage incurred during abusive grinding. The hardness of the material in the heat-affected areas and in the areas adjacent to the origins was lower than that of the surrounding tempered martensite structure. These heat-affected areas were located in the chromium plating runout plateau adjacent to the counterbore transition radius and exhibited numerous thermally induced secondary cracks. It was concluded that the cause of failure was improper overhaul process, which left grinding burns and cracks beneath the chromium coating. Subsequently, electrolyte that penetrated through these cracks promoted the formation of pits beneath the coating, which served as preferred sites for failure initiation.

© 2004 Elsevier Ltd. All rights reserved.

**Keywords:** Aircraft failures; Stress corrosion cracking; Non-destructive testing; Design; Landing gear

---

\* Corresponding author. Tel.: +972 3 640 7384; fax: +972 3 640 7617.  
E-mail address: [neliaz@eng.tau.ac.il](mailto:neliaz@eng.tau.ac.il) (N. Eliaz).

## 1. Introduction

This paper is based on failure analyses of two truck beams from the main landing gear (MLG) of a cargo aircraft due to abusive grinding following chromium plating. The MLG consists of two struts to which four-wheel bogies are mounted. The landing gear is attached to the wing and is retracted inboard into the thickened juncture of the wing and fuselage. An illustration of the assembly is given in Fig. 1.

The landing gears are being overhauled once in 10 years according to the maintenance instructions of the manufacturer. The main stages in the overhaul process include:

- (1) Sand cleaning to remove paint and rust.
- (2) Removal of the chromium plating from marked areas, followed by stress relieve heat treatment.
- (3) Use of non-destructive testing (NDT) by means of the magnetic particles technique [1].
- (4) Shot peening.
- (5) Chromium plating of the machined areas per MIL-STD-1501 (class 1, type II) [2], followed by grinding in accordance with MIL-STD-866B [3] to restore design dimensions and finish. The chromium plate runout plateau is that area of the chromium-plated surfaces where the chromium thickness changes from the required value to zero. The runout should be produced during the plating operation by use of special electrodes, current robbing, metal tape and shields, to provide a proper gradual runout (over a distance of about 2 mm) without formation of a bead or a square edge. The application of a solid film lubricant on top of chromium is recommended by the manufacturer, but is not considered as mandatory. Certain users prefer to apply corrosion prevention compounds (CPCs) to the interior of the truck beam after washing.
- (6) Stress relieve heat treatment.
- (7) Cadmium plating of the rest areas per MIL-STD-870 (type III) [4], followed by heat treatment to release hydrogen.

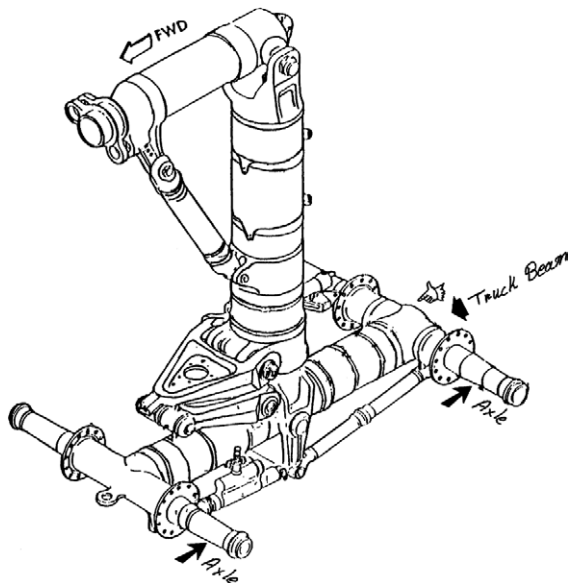


Fig. 1. Illustration of the main landing gear assembly on the subject aircraft. A finger marks the region of failure.

While a wheel was being replaced on the subject aircraft, a crack was found on the rear axle bore of the left-hand (L/H) MLG truck beam. One year later, while the same aircraft was being parked, two loud bangs (40 min apart) were heard coming from the right-hand (R/H) MLG. The landing gears from both events had been overhauled together. Upon inspection, the R/H truck beam was found cracked longitudinally at two locations on the rear axle bore (Fig. 2). No collapse or collateral damage to other structure resulted. Sections containing crack fracture surface segments from both truck beams were selected for failure analysis, which included visual examination, NDT, material characterization (namely, chemical analysis, hardness testing and metallography), and analysis of fracture surfaces by scanning electron microscopy (SEM) and X-ray energy dispersive spectroscopy (EDS).

## 2. Results and discussion

Visual examination of the R/H truck beam revealed no mechanical damage either in vicinity to the failure region or on the chromium plating. Macroscopic examination of the fracture surfaces revealed ratchet marks propagating from two origins beneath the chromium plating at two opposite locations on the outer wall of the axle (bore). The crack propagation path is shown schematically in Fig. 3. Around the origins, dark brown beachmark patterns were observed (Fig. 4).

The cracks emanating from the two origins in the R/H truck beam (see Fig. 2) were opened in the lab and studied by SEM. Metallographic inspection showed that the chromium plating was nonuniform in thickness, varying between 280 and 120  $\mu\text{m}$  within the runout plateau, where both crack origins were located (Fig. 5). Fractographic observations showed that the crack surface was consisted of two concentric thumbnail-shaped beachmarks zones – an inner small dark zone extending to approximately 0.3 mm from the bore surface, and a surrounding brighter zone extending to nearly 2.5 mm. Higher magnification revealed that the inner beachmarks zone was consisted of chemical etching features characteristic of corrosion (Fig. 6). The outer beachmarks zone exhibited a coarse, grainy topography of intergranular separation (Fig. 7). The last portion of the fracture surface (not shown in Fig. 5) was characterized by rupture dimples and quasi-cleavage surfaces characteristic of overload failure.

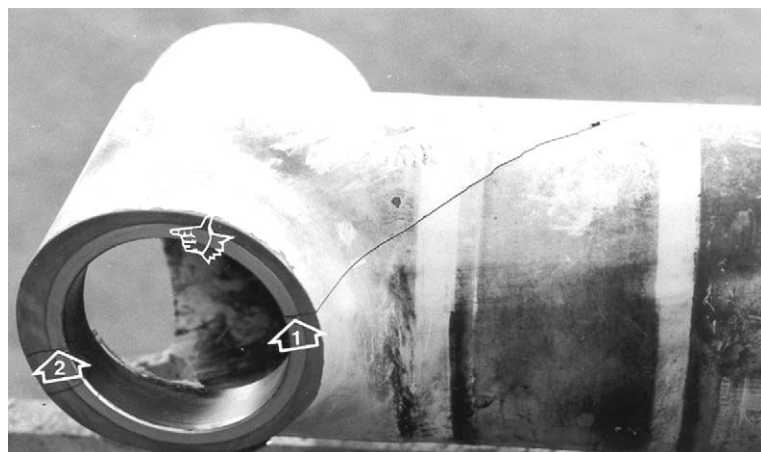


Fig. 2. Macroscopic view of the rear side of the R/H truck beam, revealing two crack origins (marked with arrows), one on each side of the bore.

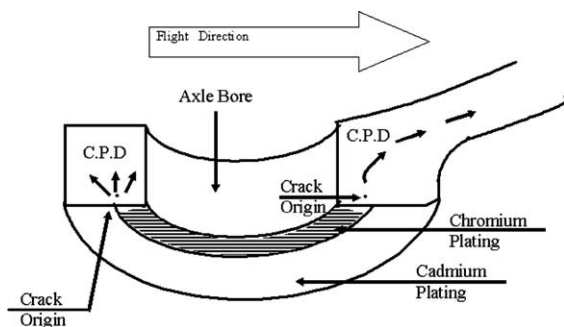


Fig. 3. Scheme of fracture. The chromium-plated zone, crack origins and fracture course are all marked.

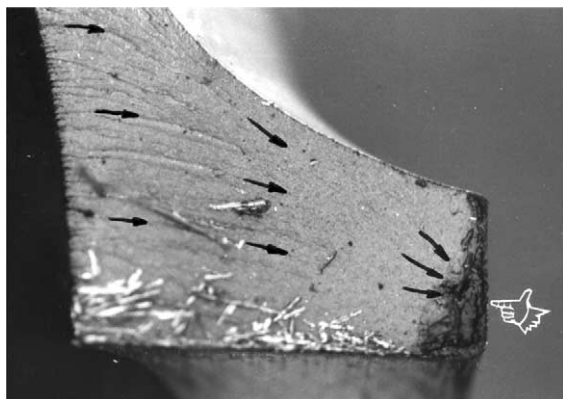


Fig. 4. Stereomicroscope image of the fracture surface around origin 1 from Fig. 2. A dark thumbnail-shaped beachmarks region near the wall is marked with finger.

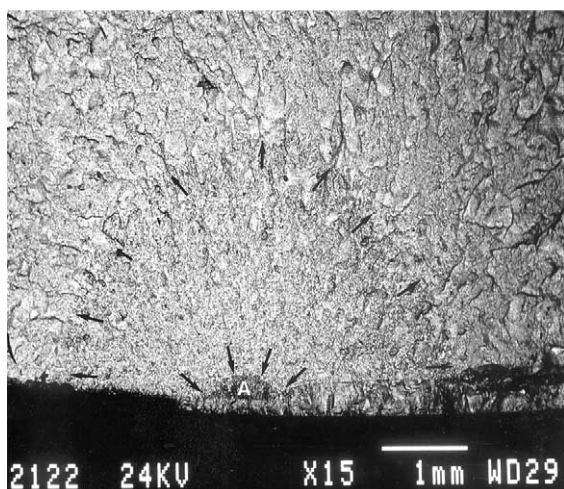


Fig. 5. SEM photomicrograph (back-scattered electrons image) showing origin 2 from Fig. 2 and its surroundings. Two thumbnail-shaped beachmarks zones are marked by arrows. The origin is located within the runout plateau where the chromium layer is thin.

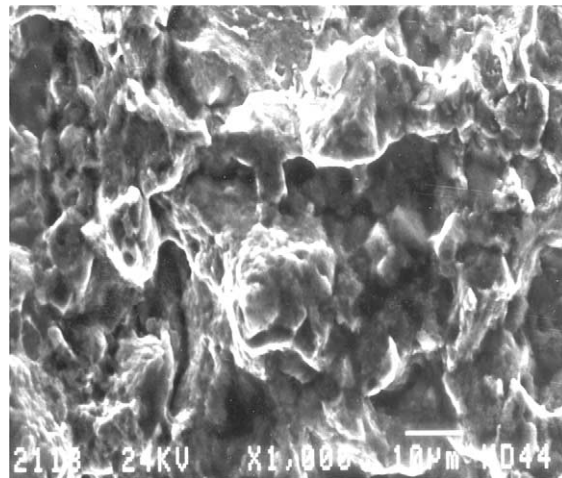


Fig. 6. SEM photomicrograph demonstrating corrosion features within the inner beachmarks zone around origin 1 from Fig. 2.

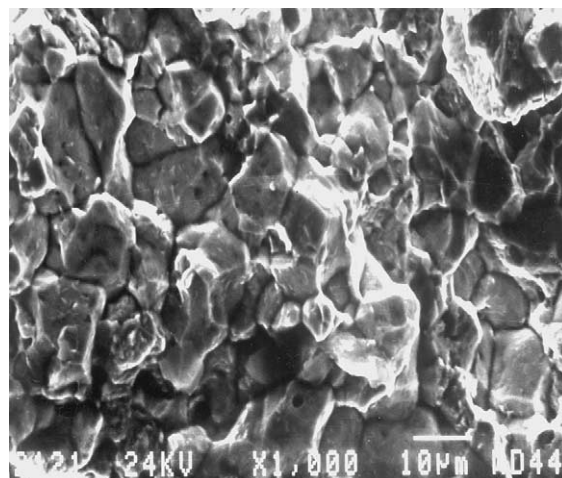


Fig. 7. SEM photomicrograph showing an intergranular fracture morphology within the outer beachmarks zone around origin 1 from Fig. 2. This morphology is typical, among other, to SCC.

Thus, it was argued that both cracks initiated from corrosion pits under the chromium plating and propagated in a stable intergranular manner, namely stress corrosion cracking (SCC, see Fig. 8 and dimensions in Table 1). Metallographic cross-section perpendicular to the crack surface through an origin further supported this argument, revealing many pits at the interface between the substrate and the chromium layer through which cracks propagated within the chromium layer. In some cases, the crack that initiated around the pit penetrated into the substrate as well (see Fig. 9). Chemical analysis (by means of EDS) at the pit area showed residues of chlorine (Cl), which may often be related to corrosion processes. Similar observations were made for the L/H truck beam, in which the crack extended from the outer bearing surface of the axle bore approximately 10.2 cm to the aft end of the longitudinal bore.

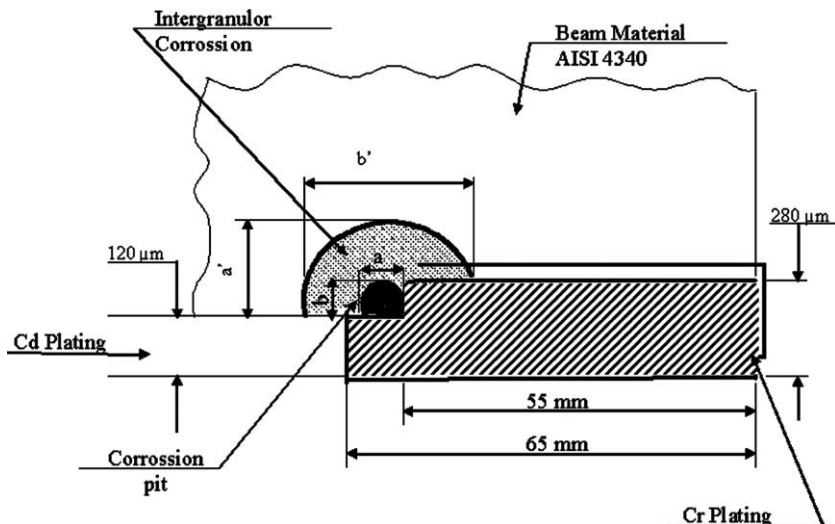


Fig. 8. Scheme of the fracture surface. The area coated with chromium, the corrosion-related pit, and the intergranular corrosion region are shown not in scale. Various dimensions are specified in Table 1.

Table 1  
Dimensions (mm) of selected features on the fracture surface (see Fig. 8)

Crack	$b$	$a$	$a'$	$b'$
1	0.7	1.7	6.3	9.5
2	0.3	0.95	3.0	4.6

In order to better understand the nature of underfilm cracking, the coating was removed around the fracture zone in the R/H truck beam, and Nital etch was carried out in accordance with MIL-STD-867 following fine sand blasting. This revealed already macroscopic areas of overtempered and untempered martensite, indicative of heat damage incurred during abusive grinding (Fig. 10(a)). These heat-affected areas were located in the chromium plating runout plateau adjacent to the counterbore transition radius, at the edge of the milling (step) zone, and exhibited numerous thermally induced secondary cracks (Fig. 10(b)). A similar condition was also observed in the same area on the bearing surface of a peace sectioned from the L/H truck beam specimen. Longitudinal heating marks could be related to the path of the grinding stone on top of the chromium layer. The microstructure of the material in the heat-affected areas and in the area adjacent to the origin of each fracture surface was consistent with overtempered martensite. The hardness of the material in these areas was lower than that of the surrounding tempered martensitic structure (Fig. 11).

During grinding much heat is generated, leading to temperature rise which might cause local martensitic transformations, volume increase, increase of residual stresses, and eventually – their release through crack initiation and propagation either into the coating or into the substrate. The high number of cracks and heating marks around the step in the runout plateau indicates that this specific area is very prone to failure as a result of grinding. The existence of a step may have a twofold effect on the local heating of the substrate. First, edge effects lead to excessive electroplate buildup; thus, more heat is generated during the grinding of the thicker chromium layer at the step region. Second, the heat conduction at a corner is much lower than that in plane. Therefore, the temperature gradient at the step area is relatively high during grinding.

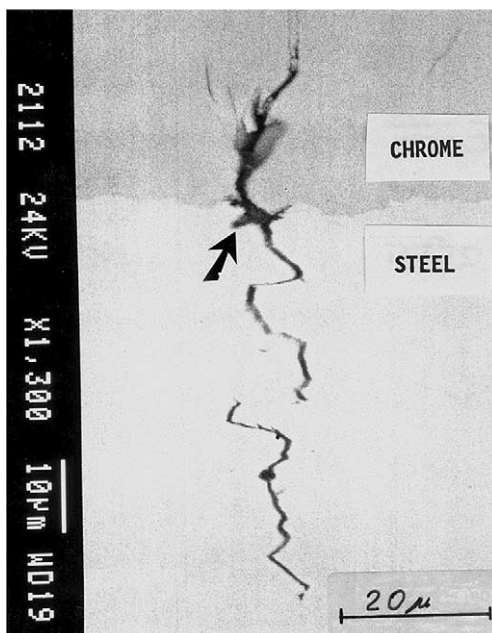


Fig. 9. Microscopic view of an area close to one of the crack origins. The metallographic cross-section was prepared perpendicular to the fracture surface. A secondary crack propagating through the chromium layer into the substrate, in parallel to the fracture surface, is evident. A corrosion pit is evident at the interface between the substrate and the coating.

Spectrochemical analysis (i.e., optic emission spectrometry) outside of the heat-affected areas verified that both truck beams were fabricated from the drawing-specified SAE 4340 alloy steel forging. Hardness measurements that were carried out on a cross-section, applying the Vickers method and a load of 10 kg, yielded values within the range 525–536 VHN. These values are equivalent to 51–52 HRC, or an ultimate tensile strength of 264–273 ksi, which satisfies the drawing requirement for a 260–280 ksi (1.80–1.93 GPa) heat treat condition. In addition, the rear axle bore outer bearing surfaces of both truck beams were shot peened.

Summarizing the data collected so far, it was concluded that cracking of the truck beams initiated near the edge of machined counterbores, around the axle bores. Chromium plating was applied at the counterbores and overlapped the outer edge onto the unmachined areas. The chromium plating was ground flat, a process which introduced high level of burns into the steel beneath the coating. These grinding burns, most likely resulting from thermal heat sink differences along the stepped surface, were probably accompanied by some cracking of the beam metal. Penetration of liquids through radial and “chicken wire” (mud) cracks in the chromium plating resulted in underfilm pitting corrosion, followed by stress corrosion crack propagation until the cracks reached a critical size, from which rapid failure occurred.

As described before, the identification of beachmark patterns, corrosion products and an intergranular fracture region, are all typical of SCC. Plane strain fracture problems in high-strength materials can be successfully treated by means of fracture mechanics approaches, mainly linear elastic fracture mechanics (LEFM) concepts, which are based on elastic stress field equations. These equations can be used if the size of the plastic zone at the crack tip is small compared to the size of the crack. The stress intensity factor,  $K$ , is a measure of the stress and strain environment of the crack. Subcritical flaw growth may occur by SCC. Given a specific material-environment interaction it is found, as in the case of fatigue crack growth, that the SCC rate (and, hence, the time to failure) is governed by  $K$ . Similar specimens with the same initial

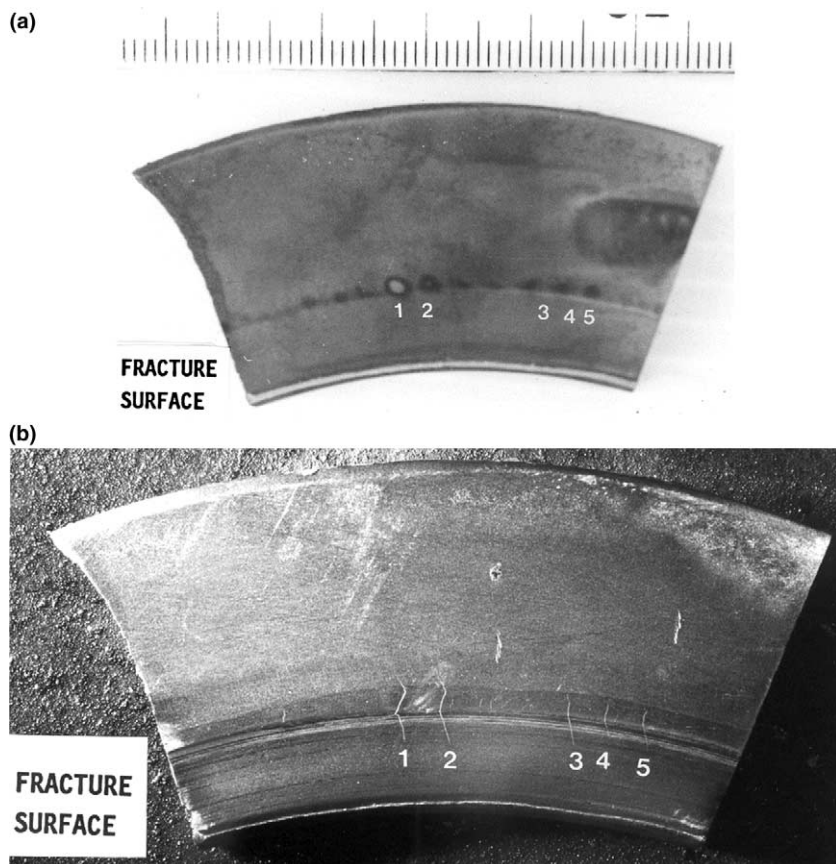


Fig. 10. View of the bearing surface of the R/H truck beam specimen: (a) areas of overtempered and untempered martensite after Nital etch. Magnification  $\sim 1.9\times$ ; (b) thermally induced cracks present in the heat-affected areas revealed by magnetic particle inspection. Magnification  $\sim 1.4\times$ .

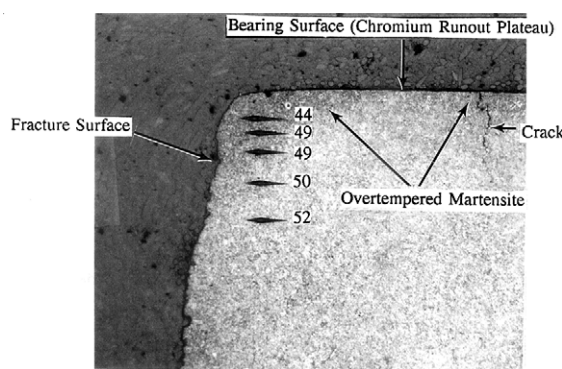


Fig. 11. Photomicrograph showing the overtempered martensitic microstructure (dark area) adjacent to the origin of the fracture surface from the L/H truck beam specimen. Microhardness Knoop measurements (values converted to HRC) were taken in this area and the surrounding normal tempered martensitic structure and are shown to the right of the indentations. Note the crack (arrow) emanating from the bearing surface in a similar overtempered martensitic area. Magnification  $\sim 100\times$ .

crack but loaded at different levels (i.e., different initial  $K$  values) show different times to failure. The specimen initially loaded to the fracture toughness,  $K_{Ic}$ , will fail immediately. It should be noted that high-strength materials, like the truck beam steel characterized herein, usually have a low value of fracture toughness. On the other hand, specimens subjected to  $K$  values below a certain threshold level, denoted as  $K_{ISCC}$ , never fail due to SCC [5].

The SAE 4340 alloy steel is known to have low resistance to uniform corrosion. Furthermore, it is susceptible to SCC in air, particularly in its hardened condition. Electrolyte penetration during service through a cracked coating might lead to formation of corrosion pits around the initial crack tip and to an increase in the stress levels around the pit until  $K_{ISCC}$  is attained. Subsequently, the crack will propagate in SCC to the final failure. Literature survey was conducted to determine the crack propagation rate ( $da/dt$ ) under SCC. While  $da/dt$  plots were found for SAE 4340 steel heat treated to 264–273 ksi and exposed to either salt water or deionized (DI) water, no data was found for the more realistic exposure to fresh air. According to the plots that were found, the time necessary to propagate the cracks to failure would be between several hours and days. Yet, in the absence of experimental data for crack propagation under fresh air, no reliable life prediction calculations were carried out for estimation of the time to failure of the truck beams under SCC.

The heating of the substrate during grinding of the chromium plating and the cracking that resulted may be attributed to improper design of the chromium plating structure. The overhaul process typically includes a magnetic particles inspection after stripping of the chromium coating, and a penetrant liquids test on the cadmium plate. Nevertheless, it was decided to examine the sensitivity of this technique for chromium plating on the failed beams before coating stripping. Severe fine radial cracking was observed in the region of the thin chromium plating. Moreover, several radial cracks penetrating through the chromium thickness were observed. After stripping of the chromium plating, the failed parts were examined again using the magnetic particles technique. Radial cracking, similar to that detected by the penetrant liquids test on top of the coating, was observed. The depth of these cracks was estimated as maximum 0.2 mm by means of the eddy current technique.

In addition to the penetrant liquids test that is required by the manufacturer, an ultrasonic technique had been developed for early reveal of beam cracking. However, such a test was carried out one week prior to the second failure event, yielding no warning. Therefore, it was decided to re-examine the effectiveness of this technique too in light of the microscopic findings of the failure analyses. As the crack propagation rate under SCC was unknown, it was decided to consider the maximum pit size observed (0.7 mm) as the size of cracks in the critical stage, or the necessary sensitivity of an effective ultrasonic technique. Indeed, it was found that the ultrasonic technique in use could not identify cracks smaller than 2.5 mm and thus was ineffective.

Review of both the manufacturer's maintenance instructions and the quality control documentation for the process of chromium electroplating on the failed beams did not indicate any problem. In addition, loading conditions and operating limits were examined. The design load condition was compared to other loads, such as take off, landing and 1 g sustained load while parked. It should be noted that all previous failures of the truck beam occurred while parked under sustained load, and that crack propagation can occur even under very low sustained loads. Under sustained load conditions, the stress around the crack is estimated to be less than 15 ksi, much below the 260 ksi ultimate tensile strength of the steel. Moreover, the location of cracks as observed in the failure analyses would not likely result in the axle separation from the truck and collapse of the gear. Hence, as cracks would likely be detected during a preflight visual inspection, safety of flight or of personnel was not considered as a major concern. Yet, the unacceptable cracking led to the following recommendations:

- (1) Proceed with penetrant liquids testing before every flight until all suspect truck beams would be replaced.
- (2) Add a magnetic particles inspection in the chromium region after its stripping, as relevant.

- (3) Define important NDT parameters previously absent in the maintenance instructions. In addition, define the necessary level of sensitivity as the highest.
- (4) Apply a routine Nital etch examination of machined chromium regions.
- (5) Eliminate the step by machining the entire surface instead of counter boring around the axle bore only. Alternatively, expand the counterbore diameter to contain the chromium plating and runout plateau entirely within the flat of the counterbore area.
- (6) Use a different grinding wheel and take precautions to avoid overheating the material. Add a caution note to start grinding from the point of thickest chromium layer. Specify 75 µm as the minimal thickness of the chromium layer at the edges.
- (7) Add a primer wipe to the chromium plated surface after grinding to seal all microcracks and those through-thickness cracks not detected by post visual inspection. This may be satisfactory to prevent electrolyte penetration.

Before concluding, it is worth noting that several years after the failure of the subject aircraft, a similar event was reported by the UK air accidents investigation branch (AAIB) [6]. In that case, the right nose-wheel stub axle of a Lockheed L1011 Tristar passenger aircraft broke. The failure developed from multi-origin cracking under the chromium plating on the SAE 4340 steel. Crack development had begun in an intergranular mode (SCC or hydrogen embrittlement), followed by a transgranular (fatigue) mode. The fracture surface had a brown or purple discoloration that was attributed to an enhanced thickness of the iron oxide layer, resulting from overheating after the cracking had begun to develop. Although metallurgical examination did not reveal any microstructural changes that would normally result from overheating during grinding, the manufacturer did detect mud-cracking pattern in the chromium adjacent to the fracture using an etching technique [7]. The manufacturer considered several non-destructive inspection techniques and concluded that there was none which, in practical terms, could be used in the field to inspect the failure location in the axle. Therefore, the company decided that the only way to ensure that any potential damage is reliably detected is to remove the axle's sleeve and chromium coating at overhaul and perform an ultra sensitive fluorescent penetrant inspection. Proper revisions were thus incorporated in the overhaul manual by June 2000 [6]. This case study implies that similar failures have occurred worldwide in different aircrafts, and that it is very important to pay the attention of both designers and overhaulers to the danger in abusive grinding of chromium (and other) plating as well as to the importance of identifying reliable early detection techniques.

### **3. Conclusions**

The results from two failure analyses of truck beams from the main landing gear (MLG) of a cargo aircraft due to abusive grinding following chromium plating were reported. The main conclusions drawn are as follows:

- (1) The beams failed by a SCC mechanism. The cracks initiated around corrosion pits beneath the chromium coating.
- (2) The corrosion pits themselves resulted from penetration of electrolyte through the cracked chromium plating and the establishment of galvanic coupling between the plating and the truck beam steel. The local corrosion was accelerated by the high cathode to anode surface areas ratio in vicinity to a pre-existing microcrack edge.
- (3) The cause of this pre-cracking of the steel substrate was improper design of the overhaul, which exposed the steel to local overheating during grinding of the chromium coating.

- (4) When the first crack in the right-hand main landing gear reached a critical size it failed catastrophically (first loud bang heard). This led to a substantial increase of the stresses acting on the second crack and to its failure (second loud bang heard).
- (5) A combination of step redesign, addition of primer and better defined inspection technique was suggested to prevent failure recurrence.

## Acknowledgements

The authors thank Itzik Cohen (IAF) for his metallurgical work, Guy Ginat (IAF) for his failure analysis work, and Baruch Tal (IAF) for his important advices.

## References

- [1] MIL-I-6868. Inspection process. Magnetic particles.
- [2] MIL-STD-1501. Chromium plating, low embrittlement, electrodeposition.
- [3] MIL-STD-866B. Grinding of chrome plated steel and steel parts heat treated to 180,000 psi or over.
- [4] MIL-STD-870. Cadmium plating, low embrittlement, electrodeposition.
- [5] Broek D. Elementary engineering fracture mechanics. The Hague, The Netherlands: Martinus Nijhoff Publishers; 1984.
- [6] Air Accidents Investigation Branch (AAIB) bulletin. UK Department of Transport (DfT); April 2000.
- [7] Messler RW, Miller RR. A new inspection process for detecting abusive grinding damage in hard chromium plated parts. Grumman Aerospace Corp., Airline Plating Forum; 1974.